



Synthesis of silver doped hydroxyapatite nanospheres using Ouzo effect

Marija Prekajski^{1,*}, Bojan Jokić², Ana Kalijadis¹, Jelena Maletaškić¹, Nadežda Stanković¹, Jelena Luković¹, Branko Matović¹

¹Vinca Institute of Nuclear Science, University of Belgrade, PO Box 522, 11001 Belgrade, Serbia

²Faculty of Technology and Metallurgy, University of Belgrade, Karnegijeva 4, 11000 Belgrade, Serbia

Received 11 March 2016; Received in revised form 15 July 2016; Accepted 20 September 2016

Abstract

Nanoemulsion technique, based on Ouzo effect, was applied for synthesis of the pure and silver doped (2.5 and 5 mol%) calcium hydroxyapatite (HAp). After calcination at 500 °C fully crystallized powders were obtained. X-ray powder diffraction analysis accompanied with Rietveld refinement revealed that the synthesized powders were single-phase hydroxyapatite. Raman spectroscopy also confirmed that the synthesized powders were single-phase. The obtained HAp particles were spherical in shape and their sizes were in the nanometer range which was revealed by field emission scanning electron microscopy analysis (FESEM). The successful synthesis of the single-phase Ag doped HAp showed that nanoemulsion method is a simple technique for obtaining pure and doped hydroxyapatite nanospheres.

Keywords: apatite, nanoparticles, nanoemulsion, Raman spectroscopy, X-ray diffraction

I. Introduction

Hydroxyapatite (denoted as HAp) belongs to a group of phosphate minerals and it is the major component of tooth enamel and bone mineral. HAp has attracted wide interest in science due to the possibility of its application as bioceramic material. Namely, hydroxyapatite has been widely used as a bone substitute and smart drug delivery due to its adequate mechanical and bioactive properties [1,2]. Properties of this material can be improved by doping that can induce complex structures at the unit cell level [3,4]. In pure CHAp Ca^{2+} ions can be replaced by various isovalent or aliovalent metal ions like Ag^+ , Sr^{2+} , Mg^{2+} , Zn^{2+} , Ce^{3+} , La^{3+} , Y^{3+} , Gd^{3+} , Tb^{3+} , etc. [3–11]. Usually, this kind of substitution leads to improvement of biological properties.

In recent years there is a constant need for development of new drugs and drug targets due to the ability of microorganisms to rapidly adapt and become resistant. The pharmaceutical companies have introduced only few new antibiotics, and none of them demonstrated improvements against multidrug-resistant bacteria [12]. That is why nanoparticles with antibacterial properties are nowadays on the top of the scientific research, as an alternative to classical antibiotics [13]. Having that

in mind, it would be interesting to develop smart drug delivery system based on HAp with antibacterial properties. Hydroxyapatite doped with small amounts of silver ions showed a broad spectrum of antibacterial activity and the absence of cytotoxicity [14–17]. Silver ions in particular show oligodynamic effect with a minimal development of microorganism's resistance [18]. Hydroxyapatites are usually doped with Ag concentrations of 0.1 to 5 mol% [16]. Studies showed that the antimicrobial effect is stronger as the concentration of Ag is higher [19], but attention must be paid not to reach cytotoxic silver concentration for the surrounding tissue [17]. That is the reason why we decided to reach 5 mol% of Ag dopant.

HAp for smart drug delivery application is mostly used as powder and its behaviour and usefulness depends on powder properties such as mean particle size, surface area and morphology. Among various methods that can be used for synthesis of Ag^+ doped HAp, nanoemulsion technique can be ideal for the fabrication of nano-biomaterials, because it provides possibility to manipulate the structure of biomaterials at the molecular level and it can produce spherical nanoparticles with small size of droplets [20,21].

Nanoemulsions represent a special class of liquid disperse systems, with droplet diameter less than 100 nm [22]. Spontaneous emulsification occurs when strongly

*Corresponding author: tel: +381 11 3408224, fax: +381 11 3408224, e-mail: prekajski@vinca.rs

hydrophobic oil is dissolved in a water-miscible solvent. This effect is nanoemulsification and it is usually called the Ouzo effect. Ouzo effect offers the possibility of obtaining dispersions without the need to use any surfactant at all, because emulsification occurs almost simultaneously in the entire volume [23].

The aim of this work was to synthesize the monophasic fully crystallized silver doped hydroxyapatite nanopowders. We have demonstrated a simple procedure for the synthesis of nanospheres of the pure and doped calcium hydroxyapatite in which 2.5 and 5 mol% of calcium is substituted with silver via a nanoemulsion route. To the best of our knowledge, this is the very first time that this method was used for the synthesis of doped HAp.

II. Experimental methods

HAp nanospheres were synthesized using analytical grade $\text{Ca}(\text{NO}_3)_2 \cdot 4\text{H}_2\text{O}$ (Riedel-de Haën, 99% purity) and $(\text{NH}_4)_2\text{HPO}_4$ (Riedel-de Haën, 99% purity). The solvent used for making nanoemulsions was analytical grade acetone. The synthesis process is illustrated in Fig. 1. An acetone solution of $\text{Ca}(\text{NO}_3)_2 \cdot 4\text{H}_2\text{O}$ was mixed with an aqueous solution of $(\text{NH}_4)_2\text{HPO}_4$ at a molar ratio of $\text{Ca}^{2+} : \text{PO}_4^{3-} = 1.67 : 1$ using a magnetic stirrer. For the preparation of the pure hydroxyapatite 1.67/100 mole of $\text{Ca}(\text{NO}_3)_2 \cdot 4\text{H}_2\text{O}$ was dissolved in 50 ml of acetone and then mixed with the 1/100 mole of $(\text{NH}_4)_2\text{HPO}_4$ which was dissolved in 50 ml of water (the ratio of acetone and aqueous solution phases in nanoemulsion was 1 : 1). The pH in the $(\text{NH}_4)_2\text{HPO}_4$ aqueous solution was adjusted to 11 with sodium hy-

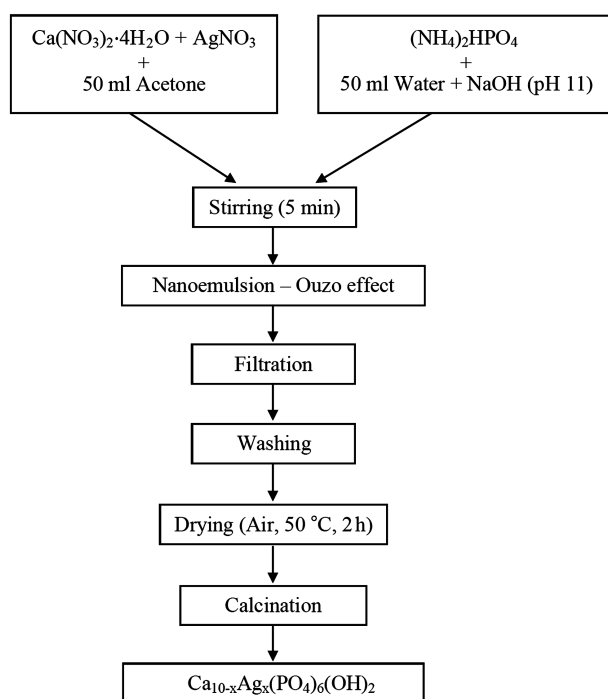


Figure 1. Synthesis procedure for obtaining Ag^+ doped HAp nanospheres using the nanoemulsion technique

droxide (1 M) prior to mixing. In case of Ag^+ doped hydroxyapatite, AgNO_3 (Sigma-Aldrich, 99% purity) was added in acetone solution of $\text{Ca}(\text{NO}_3)_2 \cdot 4\text{H}_2\text{O}$ in concentration of $(\text{Ag}/\text{Ag}+\text{Ca}) \cdot 100\% = 2.5$ and 5 mol%. The mixed solutions were stirred for 5 min. No surfactant was used in all synthesis processes. The resultant nanoprecipitates in the solutions were immediately filtered using a vacuum filtration set to avoid particle agglomeration and then washed three times using ultra-pure deionized water. The slurry of nanoprecipitates was dried out in the oven at 70°C . Finally, the obtained powders were calcined at different temperatures in order to obtain fully crystallized samples.

The phase purity and crystallinity of the produced apatite powders were examined using X-ray diffraction (Ragaku Ultima IV, Japan) and Raman spectroscopy. The X-ray beam was nickel-filtered $\text{CuK}\alpha_1$ radiation ($\lambda = 0.1540\text{ nm}$, operating at 40 kV and 40 mA). XRD data were collected from 5 to 90° (2θ) at a scanning rate of $5^\circ/\text{min}$. A refinement of the structure of calcium hydroxide phosphate was undertaken in order to elucidate the crystal structure and microstructure of hydroxyapatite. Phase analysis accompanied with Rietveld refinement was done by using the PDXL2 software (version 2.0.3.0 - Rigaku Corporation, Japan), with reference to the patterns of the International Centre for Diffraction Database (ICDD) PDF-2 Database, version 2012. Calculation of the average crystallite size (D) was performed on the basis of the full width at half maximum intensity (FWHM) of the reflections by using Scherrer's formula [24]:

$$D_{hkl} = \frac{0.9\lambda}{\beta \cdot \cos \theta} \quad (1)$$

where λ is the wavelengths of the X-rays, θ is diffraction angle, β is corrected half-width for instrumental broadening $\beta = (\beta_m - \beta_s)$, β_m observed half-width and β_s is half-width of the standard CeO_2 sample.

Raman spectra were taken with an Advantage 532 Raman spectrometer (DeltaNu Inc.) by a frequency doubled diode pumped YAG type laser operating at 532 nm.

The morphology of the obtained nanoprecipitates was studied by field emission scanning electron microscopy (FESEM) TESCAN Mira3 XMU, with electron energies of 20 kV in high vacuum. The samples used for SEM characterization were coated with 5 nm thin layer of Au/Pd using a standard sputtering technique.

III. Results and discussion

3.1. XRPD characterization

Typical X-ray diffraction patterns for the as-synthesized samples as well as the samples calcined at 500 and 900°C are shown in Fig. 2. All diffraction peaks of both samples can be well indexed to the hexagonal hydroxyapatite (ICSD Card No.: 26204). There are no other characteristic peaks of impurities or sec-

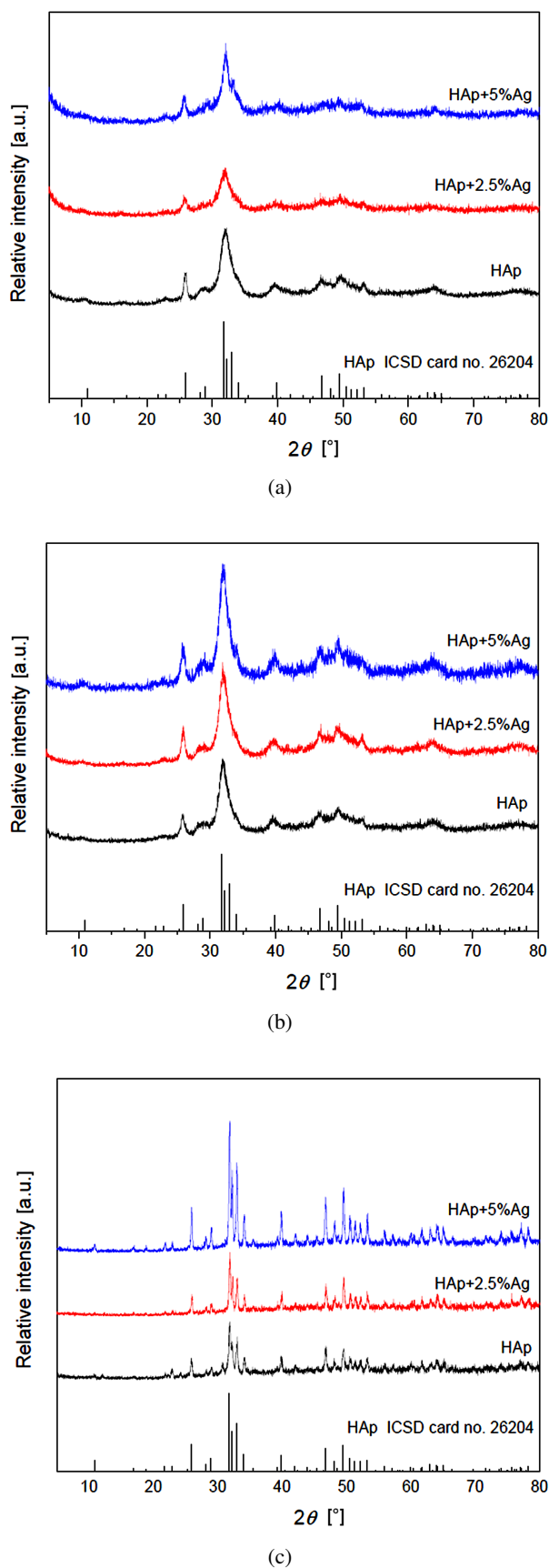


Figure 2. XRD patterns of pure and Ag^+ doped HAp samples, calcined at different temperatures: a) as-synthesized (70 °C), b) 500 °C and c) 900 °C

ondary phases, such as CaO , Ag_2O or silver phosphates. The absence of other phases in XRD pattern of Ag^+ doped HAp samples demonstrates that the Ag^+ ions have successfully substituted Ca^{2+} ions without affecting the crystal structure of the original HAp. This result is in agreement with previous studies conducted by Shirkhazadeh *et al.* [25] and Ravindran *et al.* [26].

The XRD pattern of the as-synthesized samples (Fig. 2a) revealed that the HAp phase was already forming at low temperature. However peaks are significantly broadened indicating poor crystallinity and small crystallite size. According to calculation based on the Scherrer's equation crystallite size of the as-synthesized samples is about 4 nm (Table 1). Calcination at 500 °C for 2 hours promotes process of crystallization (Fig. 2b) and crystals grow to the size of 7 nm (Table 1). Since the peaks are still very broad we decided to increase calcination temperature to 900 °C. At this temperature all samples are fully crystallized and reflections are well defined by the sharp peaks (Fig. 2c). There is still no indications of any secondary phases in Ag doped samples while the crystallites sizes grow to 19 nm (Table 1).

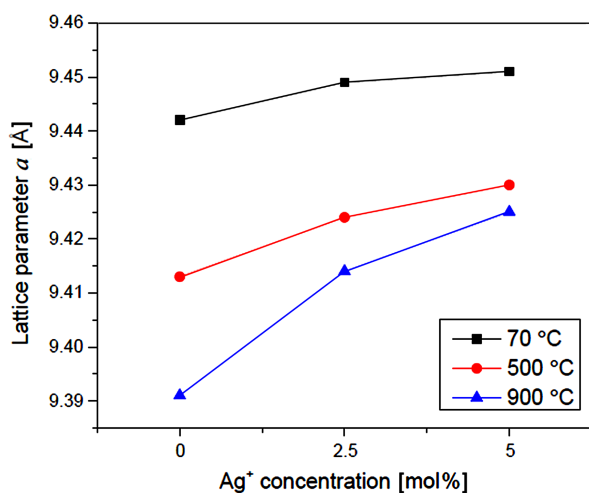
Refined unit cell parameters of all samples are presented in Fig. 3. Doping of Ag^+ ions into the apatite shows an increase in a and c lattice parameters (Fig. 3). An expansion of these lattice parameters are caused by the substitution of smaller radius ion of the Ca^{2+} (0.099 nm) by the larger Ag^+ (0.128 nm) ion. These results are in accordance with previous reports by Rameshbabu *et al.* [27] which assumed that silver substitute for calcium in the HAp lattice. On the other hand, strain in crystal lattice remains almost the same at all temperatures, but it depends on the concentration of Ag^+ in the samples. Namely, incorporation of larger ion provokes additional stress and strain in crystal structure (Table 1).

3.2. Raman spectral studies

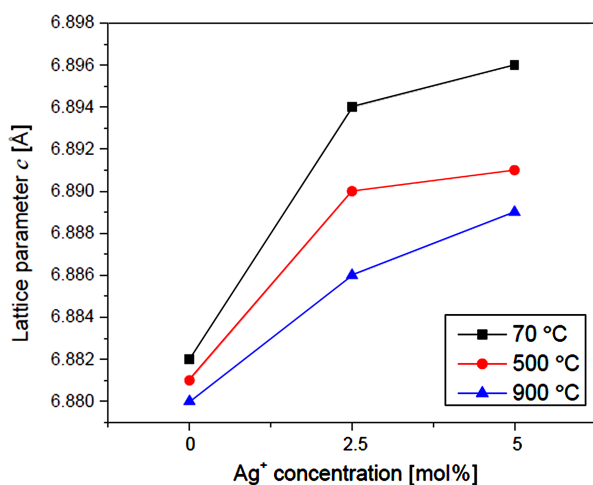
Raman analysis was used in order to verify the presence of pure HAp phase in samples, because it is known that Raman spectroscopy method is more sensitive on the presence of secondary phases than X-ray powder diffraction. Raman spectrum of HAp sample doped with higher concentration of Ag^+ is shown in Fig. 4. For comparison Raman spectrum of the pure as-synthesized sample is also represented at Fig. 4. The most intensive mode near 950 cm^{-1} is assigned to the internal modes of the PO_4^{3-} tetrahedral ν_1 frequency which corresponds to the symmetric stretching of P–O bonds [13,28]. The bands present near 1027 cm^{-1} , 1050 cm^{-1} , and 1080 cm^{-1} can be assigned to the asymmetric ν_3 (P–O) stretching [19]. The other expected bands near 576 , 590 and 616 cm^{-1} which originate from ν_4 PO_4 and bands near 430 (ν_2) and 450 cm^{-1} (ν_2) attributed to the O–P–O bending modes have weak intensities and were not detected [29,30]. The reason for such behaviour may lie in water vibrational modes, which gives rise to weak intensity stretching and bending bands in Raman spectra

Table 1. Refined microstructural factors: crystallite size (D) and strain (ϵ)

Temperature	0 mol%		2.5 mol%		5 mol%	
	D [nm]	ϵ [%]	D [nm]	ϵ [%]	D [nm]	ϵ [%]
70 °C	4.1	0.4	3.9	0.41	4.2	0.45
500 °C	6.6	0.2	6.8	0.4	6.9	0.59
900 °C	18.6	0	19.8	0.39	19.2	0.48



(a)



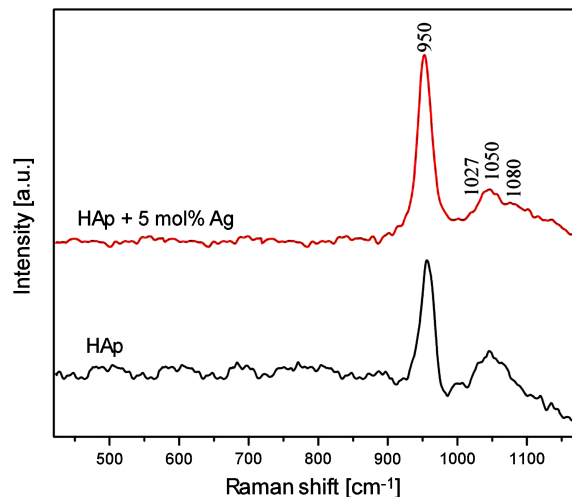
(b)

Figure 3. Refined lattice parameters a (a) and c (b) of pure and Ag⁺ doped HAp samples, calcined at different temperatures

[31,32]. The OH⁻ vibrational bands expected in the region of 630 cm⁻¹ are not clearly detected. This behaviour is in good agreement with the previous studies [33].

3.3. Morphology characterization

SEM micrographs of the pure and Ag-doped HAp powders calcined at 500 °C are shown in Fig. 5. The results showed that the obtained hydroxyapatite powders were composed of nearly spherical particles of narrow size distribution. The average particle size is about ~100 nm in all samples. Individual spheres are agglomerated and a lot of porosity is present. The formation of spherical HAp nanoparticles is due to the Ouzo ef-

**Figure 4. Raman spectra of pure and Ag⁺ doped HAp samples calcined at 500 °C**

fect which occurs in present synthesis method [34]. The material with this microstructural and texture properties have an advantage due to its application as bioceramic materials [20].

IV. Conclusions

The nanoemulsion method has been found to be very promising for the synthesis of spherical nanoparticles of the pure and Ag⁺ doped hydroxyapatite. Significant concentration of Ag⁺ ions (5 mol%) were completely incorporated in HAp lattice without formation of any impurities or secondary phases which was confirmed both by XRD and Raman analysis. Calcination at higher temperatures promotes crystallization process and crystallite growth. Incorporation of larger Ag⁺ ion instead of Ca²⁺ ion causes increase of lattice parameters. The silver ions cause the increase in the size of the crystallites in the doped samples. The synthesized nanoparticles were spherical in shape and their sizes were in the range of ~100 nm. The obtained results give new perspective for possible application of smart drug delivery in form of HAp nanospheres improved with Ag⁺ ions which has antibacterial properties.

Acknowledgements: Financial support from the Serbian Education and Science Ministry in the Framework of projects No. 45012 is gratefully acknowledged.

References

1. L.L. Hench, J. Wilson, "Surface active biomaterials", *Science*, **226** (1984) 630–636.

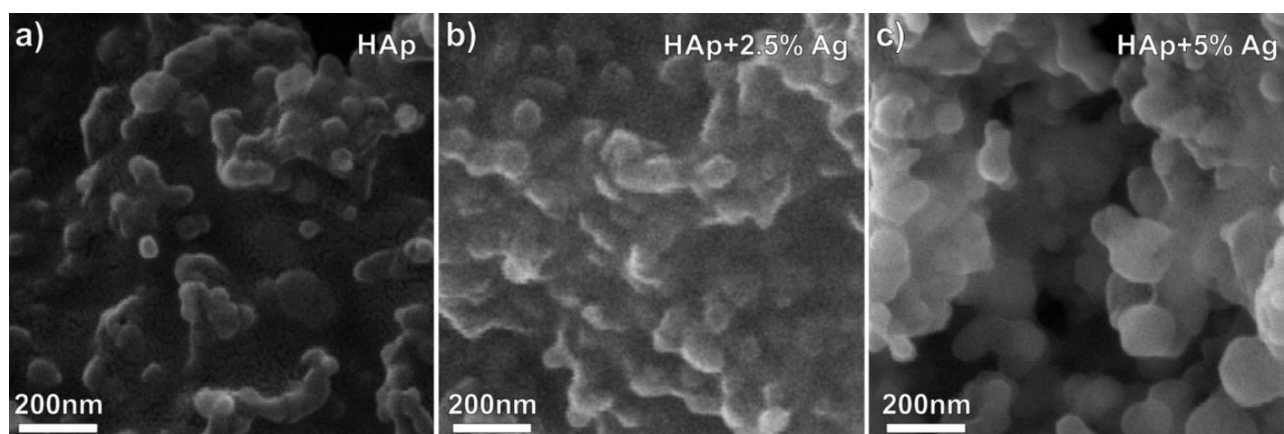


Figure 5. SEM images of samples calcined at 500 °C: a) pure HAp, b) HAp doped with 2.5 mol%, and c) HAp doped with 5 mol% Ag⁺

2. W. Paul, C.P. Sharma, “Development of porous spherical hydroxylapatite granules: Application towards protein delivery”, *J. Mater. Sci. Mater. Med.*, **10** (1999) 383–388.
3. S. Kalita, S. Bose, H. Hosick, A. Bandyopadhyay, “CaO-P₂O₅-Na₂O-based sintering additives for hydroxyapatite (HAp) ceramics”, *Biomaterials*, **25** (2004) 2331–2339.
4. A.M. Pietak, J.W. Reid, M.J. Stott, M. Sayer, “Silicon substitution in the calcium phosphate bioceramics”, *Biomaterials*, **28** (2007) 4023–4032.
5. L.T. Bang, K. Ishikawa, R. Othman, “Effect of silicon and heat-treatment temperature on the morphology and mechanical properties of silicon-substituted hydroxyapatite”, *Ceram. Int.*, **37** (2011) 3637–3642.
6. R.V. Suganthi, K. Elayaraja, M.I. Ahymah Joshy, V. Sarath Chandra, E.K. Girija, S. Narayana Kalkura, “Fibrous growth of strontium substituted hydroxyapatite and its drug release”, *Mater. Sci. Eng. C*, **31** (2011) 593–599.
7. J.T. Webster, A. Elizabeth, M. Schuleter, L.J. Smith, B.E. Slamovich, “Osteoblast response to hydroxyapatite doped with divalent and trivalent cations”, *Biomaterials*, **25** (2004) 2111–2121.
8. M.I. Ahymah Joshy, K. Elayaraja, R.V. Suganthi, V. Sarath Chandra, S. Narayana Kalkura, “In vitro sustained release of Amoxicillin from lanthanum hydroxyapatite nano rods”, *Curr. Appl. Phys.*, **11** (2011) 1100–1106.
9. A. Yasukawa, K. Kandori, H. Tanaka, K. Gotoh, “Preparation and structure of carbonated hydroxyapatite substituted with heavy rare earth ions”, *Mater. Res. Bull.*, **47** (2012) 1257–1263.
10. A. Yasukawa, K. Gotoh, H. Tanaka, K. Kandori, “Preparation and structure of calcium hydroxyapatite substituted with light rare ions”, *Colloids. Surf. A*, **393** (2012) 53–59.
11. C. Yang, P. Yang, W. Wang, J. Wang, M. Zhang, J. Lin, “Solvothetmal synthesis and characterization of Ln (Eu³⁺, Tb³⁺) doped hydroxyapatite”, *J. Colloid Interface Sci.*, **328** (2008) 203–210.
12. J.M. Conlon, J. Kolodziejek, N. Nowotny, “Antimicrobial peptides from ranid frogs: taxonomic and phylogenetic markers and a potential source of new therapeutic agents”, *Biochim. Biophys. Acta.*, **1696** (2004) 1–14.
13. C.S. Ciobanu, S.L. Iconaru, P.L. Coustumer, L.V. Constantin, D. Predoi, “Antibacterial activity of silver-doped hydroxyapatite nanoparticles against gram-positive and gram-negative bacteria”, *Nanoscale. Res. Lett.*, **7** [1] (2012) 324.
14. Ž. Radovanović, B. Jokić, Dj. Veljović, S. Dimitrijević, V. Kojić, R. Petrović, Dj. Janačković, “Antimicrobial activity and biocompatibility of Ag⁺- and Cu²⁺- doped biphasic hydroxyapatite/ α -tricalcium phosphate obtained from hydrothermally synthesized Ag⁺- and Cu²⁺- doped hydroxyapatite”, *Appl. Surf. Sci.*, **307** (2014) 513–519.
15. S. Jadalannagari, K. Deshmukh, S.R. Ramanan, M. Kowshik, “Antimicrobial activity of hemocompatible silver doped hydroxyapatite nanoparticles synthesized by modified sol-gel technique”, *Appl. Nanosci.*, **4** (2014) 133–141.
16. V. Stanic, D. Janackovic, S. Dimitrijevic, S.B. Tanaskovic, M. Mitric, M.S. Pavlovic, A. Krstic, D. Jovanovic, S. Raicevic, “Synthesis of antimicrobial monophase silverdoped hydroxyapatite nanopowders for bone tissue engineering”, *Appl. Surf. Sci.*, **257** (2011) 4510–4518.
17. A. Peetsch, C. Greulich, D. Braun, C. Stroetges, H. Rehage, B. Siebers, M. Köller, M. Eppele, “Silver-doped calcium phosphate nanoparticles: Synthesis, characterization, and toxic effects toward mammalian and prokaryotic cells”, *Colloids Surfaces B: Biointerfaces*, **102** (2013) 724–729.
18. S.L. Percival, P.G. Bowler, D. Russell, “Bacterial resistance to silver in wound care”, *J. Hosp. Infect.*, **60** (2005) 1–7.
19. M. Turkoz, A. O. Atilla, Z. Evis, “Silver and fluoride doped hydroxyapatites: Investigation by microstructure, mechanical and antibacterial properties”, *Ceram. Int.*, **39** (2013) 8925–8931.
20. M. Chorny, I. Fishbein, H.D. Danenberg, G. Golomb, “Lipophilic drug loaded nanospheres pre-

- pared by nanoprecipitation: Effect of formulation variables on size, drug recovery and release kinetics”. *J. Control. Release.*, **83** (2002) 389–400.
21. W.Y. Zhou, M. Wang, W.L. Cheung, B.C. Guo, D.M. Jia, “Synthesis of carbonated hydroxyapatite nanospheres through nanoemulsion”, *J. Mater. Sci. Mater. Med.*, **19** (2008) 103–110.
 22. M. Yu Koroleva, E.V. Yurtov, “Nanoemulsions: the properties, methods of preparation and promising applications”, *Russ. Chem. Rev.*, **81** (2012) 21–43.
 23. M. Prekajski, M. Mirković, B. Todorović, A. Matković, M. Marinović-Cincović, J. Luković, B. Matović, “Ouzo effect - New simple nanoemulsion method for synthesis of strontium hydroxyapatite nanospheres”, *J. Eur. Ceram. Soc.*, **36** [5] (2016) 1293–1298.
 24. P. Scherrer, “Bestimmung der Grösse und der inneren Struktur von Kolloidteilchen mittels Röntgenstrahlen”, *Gött Nachr*, **2** (1918) 98–100.
 25. M. Shirkhanzadeh, M. Azadegan, G.Q. Liu, “Bioactive delivery systems for the slow release of antibiotics: incorporation of Ag⁺ ions into micro-porous hydroxyapatite coatings”, *Mater. Lett.*, **24** (1995) 7–12.
 26. A. Ravindran, A. Singh, A.M. Raichur, N. Chandrasekaran, A. Mukherjee, “Studies on interaction of colloidal Ag nanoparticles with bovine serum albumin (BSA)”, *Colloid. Surface. B*, **76** (2010) 32–37.
 27. N. Rameshbabu, T.S.S. Kumar, T.G. Prabhakar, V.S. Sastry, K.V.G.K. Murty, K.P. Rao, “Antibacterial nanosized silver substituted hydroxyapatite: synthesis and characterization”, *J. Biomed. Mater. Res.*, **80A** (2007) 581–591.
 28. C.S. Ciobanu, S.L. Iconaru, P.L. Coustumer, D. Predoi, “Vibrational investigations of silver-doped hydroxyapatite with antibacterial properties”, *J. Spectroscopy*, **2013** (2013) 471061.
 29. A. Mortier, J. Lemaitre, P.G. Rouxhet, “Temperature programmed characterization of synthetic calcium-deficient phosphate apatites”, *Thermochim. Acta.*, **143** (1989) 265–282.
 30. J. Elliot, *Structural and Chemistry of Apatites and other Calcium Orthophosphates*, Amsterdam, Elsevier, 1994.
 31. A. Costescu, C.S. Ciobanu, S.L. Iconaru, R.V. Ghita, C.M. Chifiriuc, L.G. Marutescu, D. Predoi, “Fabrication, characterization, and antimicrobial activity, evaluation of low silver concentrations in silver-doped hydroxyapatite nanoparticles”, *J. Nanomater.*, **2013** (2013) 194854.
 32. C.L. Popa, C.S. Ciobanu, G. Voicu, E. Vasile, M.C. Chifiriuc, S.L. Iconaru, D. Predoi, “Influence of thermal treatment on the antimicrobial activity of silver-doped biological apatite”, *Nanoscale Res. Lett.*, **10** (2015) 502.
 33. B.O. Fowler, “Infrared studies of apatites. I. Vibrational assignments for calcium, strontium, and barium hydroxyapatites utilizing isotopic substitution”, *Inorg. Chem.*, **13** [1] (1974) 194–207.
 34. F. Ganachaud, J.L. Katz, “Nanoparticles and nanocapsules created using the Ouzo effect: Spontaneous emulsification as an alternative to ultrasonic and high-shear devices”, *Chem. Phys. Chem.*, **6** (2005) 209–216.